

# EFFECT OF NANOSILICA AND NANOBOEHMITE ON THE PYROPLASTIC DEFORMATION OF A PORCELAIN TILE BODY

**Vicente De Lorenzi, Nikelli Rabelo, Alexandre Gonçalves Dal-Bó, Michael Peterson, Adriano Michael Bernardin**

**Graduation Program in Materials Science and Engineering, PPGCEM, University of the Extreme South of Santa Catarina, UNESC, Criciúma, 88806-000, Santa Catarina, Brazil**

## ABSTRACT

Porcelain tiles are ceramic coverings with low porosity ( $WA < 0.5\%$ ) formed by a mixture of clay minerals, quartz and feldspars and fired at temperatures close to 1200 °C. During sintering, the liquid phase can result in unwanted pyroplastic deformations. In addition, rectangular formats, large dimensions, reduced thicknesses and fast thermal cycles worsen the deformations. Therefore, in this study, silica and boehmite-based nanoparticles were used to reduce the pyroplastic deformation in porcelain tiles. Ten compositions were studied using mixture design (DoE), where the raw materials, nanosilica and nanoboehmite were the factors, independent variables. The response, dependent variable, was the pyroplastic deformation. The chemical composition of the raw materials and the size and specific surface area of the nanoparticles were determined. The pyroplastic index was analyzed by ANOVA and response surfaces, showing the effect of nanoparticles on the pyroplastic deformation of porcelain tiles. The composition with the lowest pyroplasticity index in comparison to the standard was processed in an industrial kiln. The pyroplasticity index was determined and evaluated by Tukey's test. After firing, the composition was analyzed by XRD and was quantified by the Rietveld method. Rational analysis was performed to estimate the glass phase and activation energy. As a result, there was 23.8% reduction in the pyroplastic index of the porcelain tile composition at 1210 °C when 5 wt.% nanoboehmite was added to the body. The chemical composition of the glass phase showed the strongest effect on the pyroplastic index of the samples. The activation energy before the maximum densification of the samples increased by 43.8%, therefore forming a higher energy barrier against the deleterious effects of pyroplastic deformation.

## 1. INTRODUCTION

Thermal transformations in porcelain tile compositions can result in high-temperature deformations, commonly called pyroplasticity [1-2]. During the firing of porcelain tiles, viscous flow sintering results in the formation of a liquid phase and the tile no longer behaves as a solid. If a load is applied on the tile, a permanent deformation called pyroplastic deformation occurs [3-4].

Many authors state that the degree of deformation is a function of the apparent viscosity of the system, the applied stress as well as the chemical composition of the glass phase [4]. Under the action of a load, the silicate ions can slide over each other, causing a continuous deformation of the glass phase. Above the glass transition temperature ( $T_g$ ), interatomic bonding forces can resist the deformation but cannot prevent the viscous flow of the glass phase if the applied stress is high enough. As the temperature increases, the viscosity of the liquid phase decreases, facilitating development of viscous flow [5].

During firing in a typical roller kiln, the ceramic tiles must keep their sizes and form as they move through the kiln. However, this is increasingly difficult to achieve due to recent innovations in the manufacture of porcelain tiles, such as reduced thicknesses, large formats and very fast firing cycles. Therefore, the composition of the tiles and process parameters must be carefully selected to obtain low porosity porcelain tiles in fast firing cycles without deformation [4,6].

The degree of pyroplastic deformation is defined by the pyroplastic index (PI)(eq.1), which shows the tendency of a sample to warp during firing under specific conditions. The procedure used to determine the pyroplasticity index consists of measuring the curvature of a sample resting on two refractory supports during firing:

$$PI = \frac{4 \times h^2 \times S}{3 \times L^4} \quad \text{eq.1 [7]}$$

Where S is the maximum deformation (cm), h is the thickness of the sample (cm) and L is the distance between the supports (cm). Pyroplastic deformation happens as a function of the vitrification of the ceramic tile during firing.

Regarding nanomaterials, their peculiar characteristics and, specifically, their improved chemical reactivity can be explored to develop silicate-based ceramics with better properties. The use of nanotechnology is interesting in helping to reduce the pyroplastic deformation. For example, alumina nanoparticles have been used to produce aluminous porcelain with a higher mullitization rate, improving the strength of the final product [8].

Therefore, the aim of this work was to evaluate the addition of silica and boehmite nanoparticles on the pyroplastic deformation of a porcelain tile composition. A mixture design (DoE) was used, and the porcelain tile body, nanosilica and nanoboehmite were the main factors. The composition with the lowest pyroplastic deformation, according to the ANOVA, was then selected to perform an industrial test.

## 2. MATERIALS AND METHODS

Five raw materials were used to compose the porcelain tile body, by dry weight: clay 1 (20%), clay 2 (10%), albite 1 (20%), albite 2 (40%), and kaolin (10%). The silica and boehmite nanoparticles (NPs) were added as aqueous suspensions to promote the dispersion of the NPs in the porcelain tile composition. The suspension of nanosilica was formed by 40% solids and that of nanoboehmite by 20% solids. The chemical analysis of the raw materials and NPs was determined by X-ray fluorescence (Oxford Instruments X-Supreme 8000, molten sample). The structure of the nanoparticles was determined by X-ray diffraction (Bruker D8, CuK $\alpha$  radiation at 40 kV and 40 mA,  $\lambda=1.541 \text{ \AA}$ ,  $2\theta$  from 10 to 80°, 0.02° step at 4 s). The size and morphology of the NPs was analyzed by transmission electron microscopy, TEM, (Jeol JEM 1011), with a maximum acceleration voltage of 100 kV and a magnification range from 50 to 600,000 x.

After chemical and TEM analyses, a statistical design was used to study the influence of each nanoparticle addition and their interactions on the pyroplasticity of a porcelain tile body. Ten compositions were studied according to a simplex-centroid mixture design. Restrictions were imposed on the design (constraint limits), considering a minimum of 95% and a maximum of 100% for the porcelain body. The minimum and maximum of silica and boehmite nanoparticles were 0 and 5%, respectively (Tab.1).

Mix (wt.%)	Porcelain body	Nanosilica	Nanoboehmite
1 (Standard)	100	0	0
2	95.0	5.00	0
3	95.0	0	5.00
4	97.5	2.50	0
5	97.5	0	2.50
6	95.0	2.50	2.50
7	96.66	1.67	1.67
8	98.34	0.83	0.83
9	95.84	3.33	0.83
10	95.84	0.83	3.33

**Table 1.** Simplex-centroid mixture design for the porcelain body, nanosilica and nanoboehmite mixes (compositions)

To form the standard mix (mix 1) of porcelain tile, the raw materials were dried (110 °C, 24 h), ground (laboratory hammer mill), mixed, and stored, according to Tab.1. The nanoparticles were added to the standard mix (mix 1) by weight as aqueous suspensions. Each composition (mix) was then ground (laboratory eccentric mill, 500 mL, alumina balls) with 50 wt.% water (1.50 g/cm<sup>3</sup> density) for 45 min until a residue of 1.5-2 wt.% at 325 Tyler mesh (44  $\mu\text{m}$ ) was obtained.

The slurries were dried (110 °C, 24 h) and the dried powders were disaggregated and mixed with 6.5 wt.% water. The granulated powders were compacted by uniaxial pressing (Gabrielli LB press, 40 MPa) forming 10 mm × 80 mm × 6 mm samples. Five samples were pressed for each composition (mix) of Tab.1. The pressed samples were dried (110 °C, 24 h), placed on a refractory tray supported by their edges according to [7], and fired to determine the pyroplastic deformation.

The pressed samples (mixes of Tab.1) were fired in an electrical laboratory roller kiln (Servitech CT094) at 1190, 1200 and 1210 °C for 5 min at the maximum temperature, in a firing cycle of 50 min. The pyroplasticity index (PI) was determined for five samples of each formulation (n=5). The PI results were analyzed by multiple regression, fitting the data to the mean squares model. The validation of the model was carried out by the hypothesis test (ANOVA) and its fit by the coefficient of determination  $R^2$ .

The composition with the lowest pyroplastic index, in comparison to the standard (mix 1), was selected for production in industrial conditions. An industrial grinding, spray drying, pressing, drying and firing cycle was performed. The particle size distribution was determined by laser diffraction (CILAS 920, 0.30–400  $\mu\text{m}$ ). The specific surface area was determined by  $\text{N}_2$  adsorption (BET method, Quantachrome Nova 1200e). The pyroplasticity index was then determined at 1210 °C with the spray-dried body according to the procedure described above (refractory mold method) and was evaluated by the Tukey test. The water absorption test was performed for the fired samples according to ISO 10545-3. Densification after firing was determined in water [9]. The crystalline/glass phases formed after firing were determined by X-ray diffraction (Bruker D8 Advance) and the diffractograms were analyzed using the RIR-Rietveld method (GSAS EXPGUI) and rational analysis for the glass phase. The chemical composition of the glass phase was calculated from the overall chemical composition and from the quantification of the crystalline phases [4]. Finally, thermal behavior was determined by contact dilatometry (Netzsch DIL 402) at 5, 10 and 15 °C/min heating rates, from room temperature to the softening point of the sample. The results were used for the calculation of the activation energy by the isoconversional method [10] between 1100 to 1200 °C, which comprise the final stages of porcelain tile sintering [11].

### 3. RESULTS AND DISCUSSION

The chemical analysis of the raw materials is shown in Tab.2. The most refractory minerals are kaolin and clay 2, due to their  $\text{SiO}_2$  and  $\text{Al}_2\text{O}_3$  contents and lower alkaline oxide content in comparison to clay 1. Despite its high  $\text{Al}_2\text{O}_3$  content (27.6 wt.%), clay 1 has a higher content of  $\text{K}_2\text{O}$ ,  $\text{CaO}$  and  $\text{MgO}$  (2.4, 2.4 and 1.1 wt.%, respectively). Clay 1 exhibits 1.2 wt.% of  $\text{Fe}_2\text{O}_3$  and clay 2 exhibits 0.95 wt.%. Kaolin exhibits  $\text{K}_2\text{O}$  and  $\text{Fe}_2\text{O}_3$  (1.4 and 0.64 wt.%, respectively).

Oxides (wt.%)	Clay 1	Clay 2	Albite 1	Albite 2	Kaolin	Nanosilica	Nanoboehmite
SiO <sub>2</sub>	56.6	72.0	77.2	77.0	72.9	98.0	3.95
Al <sub>2</sub> O <sub>3</sub>	27.6	19.1	9.1	14.3	18.8	1.1	95.6
TiO <sub>2</sub>	0.09	0.16	0.07	0.04	0.12	-	-
Fe <sub>2</sub> O <sub>3</sub>	1.2	0.95	0.23	0.21	0.64	-	-
CaO	2.4	0.05	2.9	0.17	0.05	-	-
MgO	1.1	0.33	1.7	0.02	0.17	-	0.43
K <sub>2</sub> O	2.4	1.1	2.3	1.5	1.4	-	-
Na <sub>2</sub> O	2.1	0.01	2.7	5.9	0.05	0.9	-
L.O.I.	6.6	6.3	3.9	0.84	5.9	-	-

**Table 2.** Chemical compositions of the raw materials

Albites 1 and 2 contain similar amounts of SiO<sub>2</sub> and a higher amount of Na<sub>2</sub>O than K<sub>2</sub>O. They exhibit a small amount of Fe<sub>2</sub>O<sub>3</sub> than clays 1 and 2 and kaolin. They are, therefore, typical raw materials for a porcelain tile body that is processed by viscous flow sintering, resulting in low water absorption. K<sub>2</sub>O forms eutectics at lower temperatures, Na<sub>2</sub>O reduces the viscosity of the liquid phase during sintering.

The chemical analysis of the silica and boehmite nanoparticles is shown in Tab.2. Nanosilica exhibits 98 wt.% of SiO<sub>2</sub> and nanoboehmite 96 wt.% of Al<sub>2</sub>O<sub>3</sub>. Chemical analysis was performed with the dried and calcined samples. The nanosilica and nanoboehmite were available as water suspensions. The XRD analysis showed that nanosilica is amorphous (Fig.1(1)) and nanoboehmite exhibits boehmite (AlO(OH)) as the only phase (Fig.1(2)).

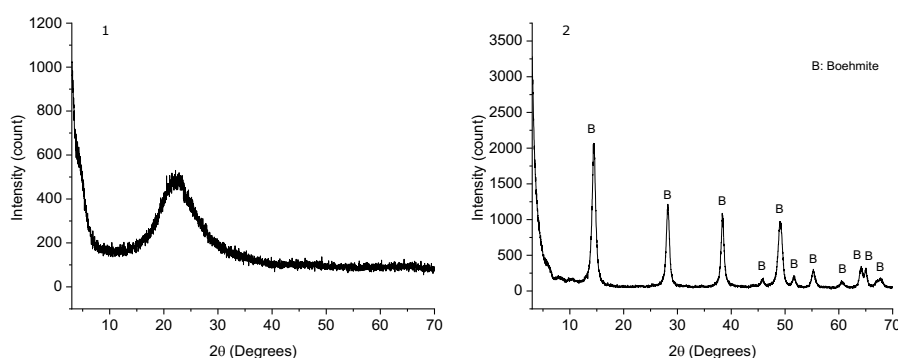


**Figure 1.** X-ray diffraction analysis of nanosilica (1) and nanoboehmite (2)

The size and morphology of the nanoparticles is shown in Fig.2(1) for nanosilica and Fig.2(2) for nanoboehmite (performed by TEM analysis). Both particles are approximately 20 nm in size. Nanosilica exhibits spherical morphology and nanoboehmite is mainly rodlike.

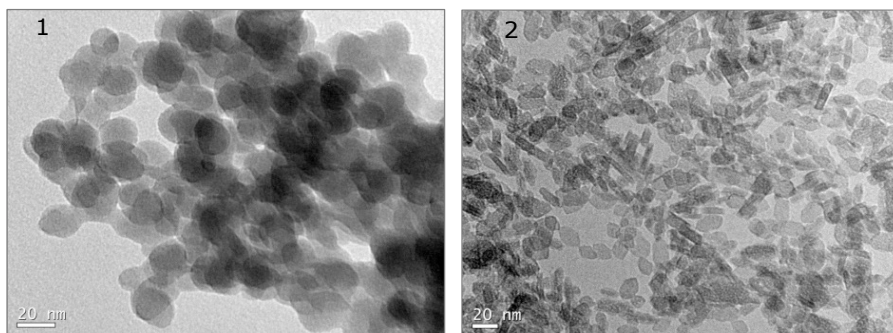


**Figure 2.** Transmission electron microscopy images of nanosilica (1) and nanoboehmite (2)

The pyroplastic index (PI) of the mixture design (Tab.1) was determined by analysis of variance (ANOVA) and the effect of nanosilica, nanoboehmite and the standard body on PI is shown as response surfaces (Fig.3). According to Tab.3, the most significant model is the cubic one, since the p-value < 0.01 for all temperatures (confidence greater than 99%) with the highest determination coefficients (R<sup>2</sup>), 87, 97 and 98% for 1190, 1200 and 1210 °C, respectively.

Pyroplastic index at 1190 °C (10 <sup>-4</sup> cm <sup>-1</sup> )									
ANOVA	Main effects			Error			Trust trials		
	SS	DF	MS	SS	DF	MS	F	p	R <sup>2</sup>
Linear	0	2	0	0	47	0	69.77	0.00	0.75
Quadratic	0	3	0	0	44	0	0.28	0.84	0.75
Special cubic	0	1	0	0	43	0	3.46	0.07	0.77
Cubic	0	2	0	0	41	0	16.67	0.00	0.87
Pyroplastic index at 1200 °C (10 <sup>-4</sup> cm <sup>-1</sup> )									
ANOVA	Efectos principales			Error			Pruebas de confianza		
	SS	DF	MS	SS	DF	MS	F	p	R <sup>2</sup>
Linear	0	2	0	0	47	0	117.36	0.00	0.83
Quadratic	0	3	0	0	44	0	23.48	0.00	0.94
Special cubic	0	1	0	0	43	0	2.81	0.10	0.94
Cubic	0	2	0	0	41	0	19.13	0.00	0.97
Índice de piroplasticidad a 1210 °C (10 <sup>-4</sup> cm <sup>-1</sup> )									
ANOVA	Efectos principales			Error			Pruebas de confianza		
	SS	DF	MS	SS	DF	MS	F	p	R <sup>2</sup>
Linear	0	2	0	0	47	0	285.15	0.00	0.92
Quadratic	0	3	0	0	44	0	11.64	0.00	0.96
Special cubic	0	1	0	0	43	0	1.64	0.21	0.96
Cubic	0	2	0	0	41	0	23.73	0.00	0.98
SS means sum of squares, DF is degrees of freedom, MS is mean square									

**Table 3.** Analysis of variance (ANOVA) for the pyroplastic index (10<sup>-4</sup> cm<sup>-1</sup>) at 1190, 1200 and 1210 °C

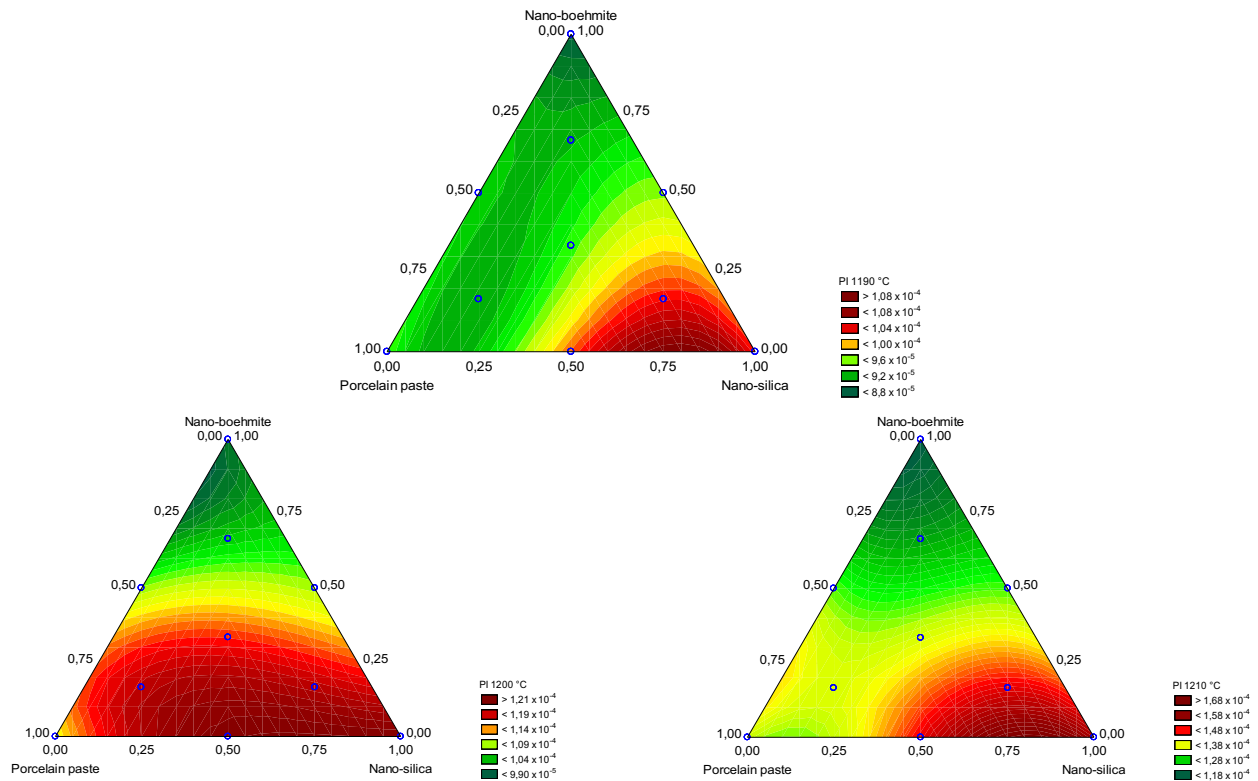


**Figure 3.** Response surfaces for the pyroplastic index (PI) 1190, 1200 and 1210 °C

The higher the nanoboehmite content, the lower the pyroplastic indices regarding the standard body (mix 1). Mixes 3, 10 and 5 (in this order) show the lowest PI for all temperatures (1190, 1200 and 1210 °C) (Fig.3). The addition of nanosilica showed an inverse effect at the same temperatures. Mixes 2, 4 and 9 stood out, agreeing with some studies [12,13] stating that the higher the quartz content in the porcelain tile composition, the more important the diffusion process to dissolve silica, which will negatively affect the precipitation of mullite. These studies also show that the finer the particle size distribution of free quartz in a composition, the greater the pyroplastic deformation. This happens because more liquid will be formed from the silica melt, resulting in less mullitization and greater pyroplastic deformation.

Regarding the effect of nanoboehmite on the pyroplastic deformation of the porcelain tile system, mix 3 was selected for an industrial test to scale up the results of the laboratory phase. The slip density, granule moisture, degree of densification after firing and water absorption of the tiles are shown in Tab.4 in comparison with the standard composition.

Grinding	Standard	Mix 3
Slip density (g/L)	1690	1675
Slip residue (45 µm) (%)	2	1.8
Spray-Drying	Standard	Mix 3
Spray-drying temperature (°C)	600	
Moisture content (%)	6.5	6.3
Homogenization time (h)	48	
Pressing	Standard	Mix 3
Reference firing size (mm)	600 × 600	
Specific pressure (kgf/cm <sup>2</sup> )	460	
Drying	Standard	Mix 3
Cycle time (min)	60	
Maximum temperature (°C)	180	
Firing	Standard	Mix 3
Cycle time (min)	33	
Maximum temperature (°C)	1238	
Densification (g/cm <sup>3</sup> )	2.296	2.303
Water absorption (%)	0.06	0.07

**Table 4.** Processing parameters of mix 3 in comparison with the standard composition

A Tukey test was performed for the pyroplastic deformation test to show the statistical differences between the standard composition and mix 3. According to the graph in Fig.4, the null hypothesis is not true and therefore the results are significant and show a 23.8% reduction (regarding the average) of the pyroplastic deformation of mix 3 when compared with the standard formulation.

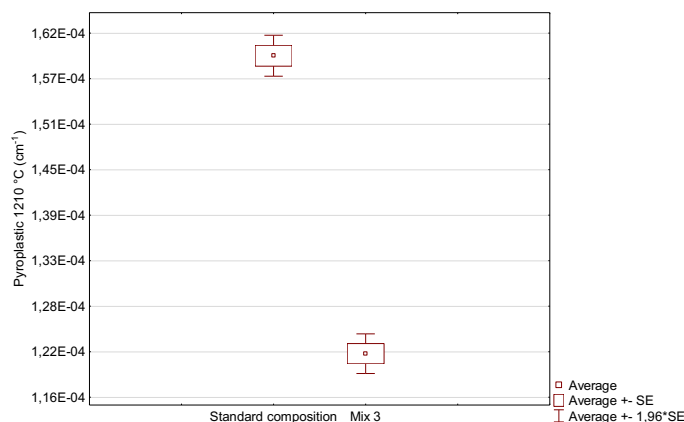


**Figure 4.** Comparison of the pyroplastic index of the standard and mix 3 at 1210 °C (SE: standard error)

The microstructure of the standard porcelain tile composition and that of mix 3 after firing was determined by X-ray diffraction and the amounts of phases were quantified by the Rietveld method (Fig.5). There were statistical differences between all phases formed (uncertainty).

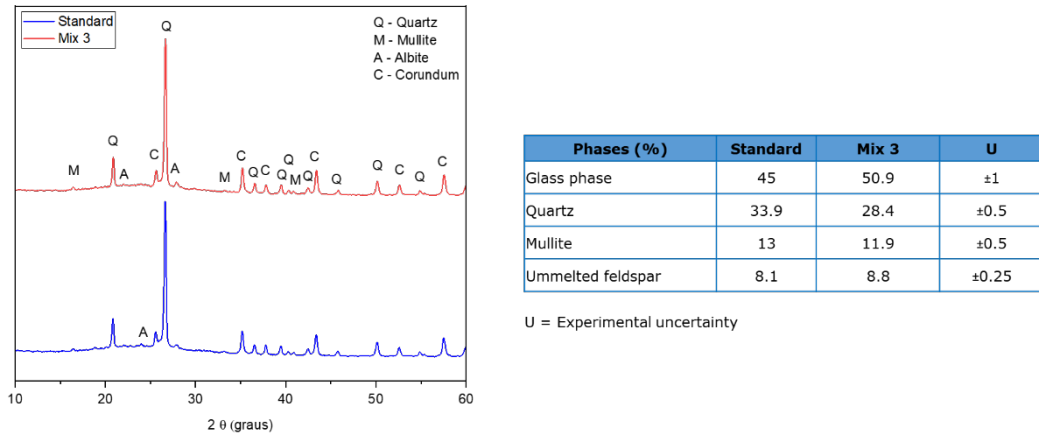


**Figure 5.** X-ray diffraction and quantification of the phases by the Rietveld method of the standard composition and mix 3

Considering the residue of mix 3 (1.8 wt.% at 44 μm), probably the particle size was determinant for the higher content of glass phase in mix 3 in comparison to the standard (at least 3.9% increase). The particle size distribution of mix 3 is finer in comparison to the standard composition (Fig.6).

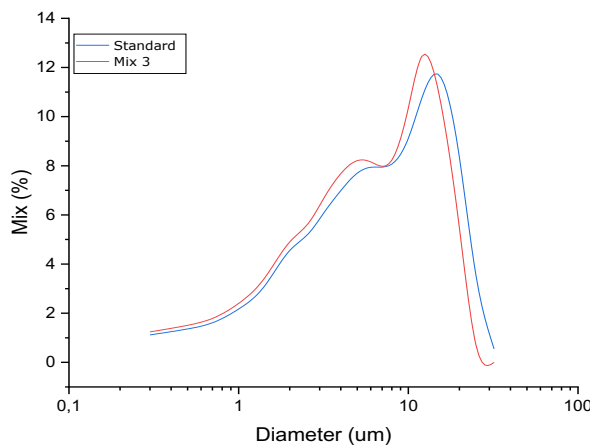


**Figure 6.** Particle distribution of the standard mix and mix 3

Mix 3 shows a higher specific surface area than the standard (Tab.5).

Mix	Specific surface area (m <sup>2</sup> /g)
Standard	6.67
Mix 3	9.50

**Table 5.** Specific surface area of standard mix and mix 3

A reduced particle size and consequent increased surface area is the driving force for the development of viscous flow sintering and formation of the glass phase [14,15]. During sintering, the glass phase will fill the voids among solid particles and therefore will reduce the porosity of the ceramic material, resulting in the densification of the tile. The nanoboehmite has also reduced the quartz content in the samples, with 4.5 less quartz in mix 3 in comparison the standard composition. The same is true for the secondary mullite precipitation [12] for mix 3, a reduction of 1% in mullite in comparison to the standard (Fig.5). The estimation of the oxide content of the glass phase for mix 3 and the standard is shown in Tab.6.

Oxides (wt.%)	Standard	Mix 3	U
SiO <sub>2</sub>	76.3	75.6	±0.5
Al <sub>2</sub> O <sub>3</sub>	7.7	10.0	±0.3
Na <sub>2</sub> O	5.9	5.4	±0.2
K <sub>2</sub> O	4.4	3.8	±0.1
CaO	3.3	3.0	±0.2
MgO	1.1	1.0	±0.2
Fe <sub>2</sub> O <sub>3</sub>	1.1	1.0	±0.2
TiO <sub>2</sub>	0.2	0.2	±0.1

**Table 6.** Chemical analysis (estimation) of the glass phase of the standard composition and mix 3 (U = experimental uncertainty)

Within the experimental uncertainty, the changes in oxide content of the glass phase for mix 3 in comparison to the standard were: Al<sub>2</sub>O<sub>3</sub> (1.7% higher), K<sub>2</sub>O (0.4% lower) and Na<sub>2</sub>O (0.1% lower). Besides the small statistical differences, K<sub>2</sub>O and Na<sub>2</sub>O are related to the unmelted feldspar content of mix 3 (8.8%) and the standard (8.1%). The difference in alumina content is justified by the addition of nanoboehmite in the mixes. Al<sup>3+</sup> ions, due to their amphoteric character, can act as lattice modifiers in octahedral coordination if there are a sufficient number of unbridged oxygens, as well as replacing Si<sup>4+</sup> ions and acting as lattice formers in tetrahedral coordination. The Si<sup>4+</sup> replacement is the most frequent effect for Al<sup>3+</sup>, reducing non-bridge oxygens and, therefore, increasing the viscosity of the melt and improving the thermal stability of glasses [16].

In glasses, the main mechanisms that influence viscosity at high temperatures (due to strong molecular vibrations) are the strength of the bonds, influenced by the chemical composition, and the degree of rupture of the glass network. The reduction of pyroplasticity of mix 3 compared to the standard could be caused by the entrance of Al<sup>3+</sup> ions in the glass phase structure in tetrahedral coordination, acting as glass formers during the viscous flow sintering of the porcelain tiles when feldspars are initially melted [17]. After complete dissolution of the feldspars, any additional alumina dissolved in the glass melt is likely to assume a coordination of 5 or greater, thus behaving as a network modifier.

In excess regarding the  $\text{Al}/(\text{Na}^+\cdot\text{K}^+\cdot\text{Ca}^{2+})$  feldspar composition, the  $\text{Al}^{3+}$  ions no longer work as glass formers, since the  $\text{Al}^{3+}$  ions cannot be compensated by the  $\text{Na}^+$ ,  $\text{K}^+$  or  $\text{Ca}^{2+}$  of the feldspars already linked to the glass structure.

Finally, to confirm the hypothesis of better thermal stability of the compositions at high temperature, the determination of the activation energy was carried out. The temperature range was 1100–1200 °C, which is the interval prior to maximum densification of porcelain tiles and in which an intense viscous flow takes place [11]. At 1100 °C, the difference in activation energy was 13.8%, rising to 46.8% difference at 1190 °C (Fig.7). Therefore, there was a higher energy barrier in mix 3 compared to that of the standard composition. At 1200 °C, the activation energy of the standard could not be measured due to its high degree of sintering.

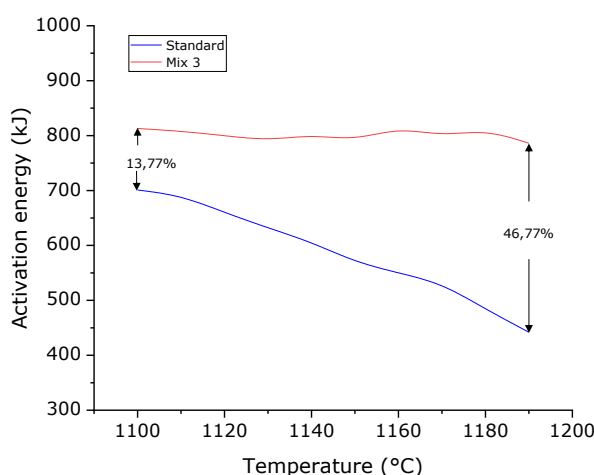


**Figure 7.** Activation energy of the standard composition and mix 3

The higher activation energy in mix 3 regarding the standard probably helped to reduce the pyroplastic deformation. The activation energies in this work agree with those in the literature [11]. The activation energies of the viscous flow at 1200 °C for porcelain tiles, calculated by the Arrhenius method, is 656.9–945.6 kJ/mol for compositions richer in sodium feldspars, and 297.1–393.3 kJ/mol for that richer in potassium feldspars. In this work, the energies were 442–815 kJ/mol for the entire range of temperatures and compositions. The mixes in this work exhibited higher content of sodium feldspars and are, therefore, consistent with the reported literature.

## 4. CONCLUSIONS

In this work, the effect of nanosilica and nanoboehmite addition on the pyroplastic deformation of a porcelain tile composition was studied using mixture design, multiple regression and response surfaces. The main conclusions are:

- The mixture design was a powerful procedure to evaluate the effect of the nanoparticles on the pyroplastic deformation of the porcelain tile composition.
- The higher content of nanosilica worsened the pyroplastic deformation of the porcelain tile standard. Probably the diffusion of silica has affected the sintering behavior of the tile composition.
- The best (lowest) pyroplastic deformation was that of the mix with 5 wt.% nanoboehmite at 1210 °C. The Tukey test showed an improvement of 23.8% (reduction in pyroplastic deformation) regarding the standard.
- By X-ray diffraction analysis a large glass phase for mix 3 was observed in comparison to the standard. The chemical composition of the glass phase plays a key role in the pyroplastic deformation.
- Due to the amphoteric nature of  $\text{Al}^{3+}$  ions they act as glass formers on the glass phase, improving the thermal stability of the composition.
- The determination of the activation energy showed an increase in the energy barrier of 43.8% at 1190 °C for mix 3 in comparison to the standard composition.

## 5. REFERENCES

- [1] Buchtel A M, Carty W M, Noirot M D, 2004. Pyroplastic deformation revisited. In *Whitewares and Materials: Ceramic Engineering and Science Proceedings* (25–42). <https://doi.org/10.1002/9780470291177.ch5>
- [2] Bresciani A, Spinelli B, 2012. Porcelain tile pyroplastic deformation during firing and post-firing variations of planarity. Germany: *Ceramic Forum International* 89, E41–E45.
- [3] Porte F, Brydson R, Rand B, Riley F L, 2004. Creep viscosity of vitreous China. *Journal of the American Ceramic Society* 87, 5, 923–928. <https://doi.org/10.1111/j.1551-2916.2004.00923.x>
- [4] Zanelli C, Raimondo M, Guarini G, Dondi M, 2011. The vitreous phase of porcelain stoneware: Composition, evolution during sintering and physical properties. *Journal of Non-Crystalline Solids* 357, 16, 3251–3260. <https://doi.org/10.1016/j.jnoncrysol.2011.05.020>
- [5] Carter C B, Norton M G, 2007. *Ceramic materials: Science and Engineering*. New York: Springer.
- [6] Carty W M, 2002. Observations on the glass phase composition in porcelains. United States: *Materials & Equipment/Whitewares: Ceramic Engineering and Science Proceedings* 23, 79–94. <https://doi.org/10.1002/9780470294734.ch22>
- [7] Melchiades F G, Boschi A O, Dos Santos L R, Dondi M, Zanelli C, Paganelli M, Mercurio V, 2014. El fenómeno de la piroplasticidad em baldosa de gres porcelánico. Castellón: Congreso Mundial de la Calidad del Azulejo y del Pavimento Cerámico, QUALICER.
- [8] Belnou F, Goeuriot D, Goeuriot P, Valdivieso F, 2004. Nanosized alumina from boehmite additions in alumina porcelain: Effect on reactivity and mullitisation. *Ceramics International* 30, 6, 883–892. <https://doi.org/10.1016/j.ceramint.2003.10.009>
- [9] Ribeiro A et al, 2020. Determinación de la densidad aparente de baldosas cerámicas utilizando agua: Validación del método. Castellón Congreso Mundial de la Calidad del Azulejo y del Pavimento Cerámico, QUALICER.
- [10] Zanelli C, Raimondo M, Guarini G, Dondi M, 2011. The vitreous phase of porcelain stoneware: Composition, evolution during sintering and physical properties. *Journal of Non-Crystalline Solids* 357, 16, 3251–3260. <https://doi.org/10.1016/j.jnoncrysol.2011.05.020>
- [11] Conceição M M, Fernandes Jr V J, Sinfronio F S M, Santos J C O, Silva M C D, Fonseca V M, Souza A G, 2005. Evaluation of isothermal kinetic of sweetener. *Journal of Thermal Analysis* 79, 2, 263–266. <https://doi.org/10.1007/s10973-005-0046-6>
- [12] Zanelli C et al, 2004. Sintering mechanisms of porcelain stoneware tiles. Castellón Congreso Mundial de la Calidad del Azulejo y del Pavimento Cerámico, QUALICER 247–259.
- [13] Riella H G, Franjndlich E U C, Durazzo M, 2002. Caracterização e utilização de fundentes em massas cerâmicas. *Cerâmica Industrial* 7, 3, 33–36.
- [14] Restrepo J J, Dinger D R, 2003. Controle da deformação piropástica em massas de porcelanas triaxiais usando a análise dilatométrica. *Cerâmica Industrial* 8, 4, 37–48.
- [15] Chakravorty A K, Ghosh D K, 1991. Kaolinite–mullite reaction series: The development and significance of a binary aluminosilicate phase. *Journal of the American Ceramic Society* 74, 6, 1401–1406. <https://doi.org/10.1111/j.1151-2916.1991.tb04119.x>
- [16] Barsoum M, 2003. *Fundamentals of ceramics*. 2<sup>nd</sup> ed. London: IOP Publishing.
- [17] Amorós J L, Orts M J, García-Ten J, Gozalbo A, Sánchez E, 2007. Effect of the green porous texture on porcelain tile properties. *Journal of the European Ceramic Society* 27, 5, 2295–2301. <https://doi.org/10.1016/j.jeurceramsoc.2006.07.005>
- [18] Navarro J M F, 1991. El estado vítreo y la estructura de los vidrios. *El Vidrio*. 2<sup>a</sup> ed. Madrid: Consejo Superior de Investigaciones Científicas 47–123.
- [19] Conte S, Zanelli C, Ardit M, Cruciani G, Dondi M, 2020. Phase evolution during reactive sintering by viscous flow: Disclosing the inner workings in porcelain stoneware firing. *Journal of the European Ceramic Society* 40, 4, 1738–1752. <https://doi.org/10.1016/j.jeurceramsoc.2019.12.030>